Journal of
Photonics for Energy

PhotonicsforEnergy.SPIEDigitalLibrary.org

Experimental demonstration of voltage-matched two-terminal tandem minimodules

Kirstin Alberi
James Moore
Kenneth Schmieder
Matthew Lumb
Robert Walters
Eric Armour
Leo Mathew
Rajesh Rao

SPIE.

Kirstin Alberi, James Moore, Kenneth Schmieder, Matthew Lumb, Robert Walters, Eric Armour, Leo Mathew, Rajesh Rao, "Experimental demonstration of voltage-matched two-terminal tandem minimodules," *J. Photon. Energy* **8**(4), 045504 (2018), doi: 10.1117/1.JPE.8.045504.

Experimental demonstration of voltage-matched two-terminal tandem minimodules

Kirstin Alberi,[a,*] James Moore,[b] Kenneth Schmieder,[c] Matthew Lumb,[b] Robert Walters,[d] Eric Armour,[e] Leo Mathew,[f] and Rajesh Rao[f]

[a]National Renewable Energy Laboratory, Golden, Colorado, United States
[b]George Washington University, Washington, DC, United States
[c]Naval Research Laboratory, Washington, DC, United States
[d]Formerly with Naval Research Laboratory, Washington, DC, United States
[e]Veeco MOCVD, Somerset, New Jersey, United States
[f]Applied Novel Devices, Austin, Texas, United States

Abstract. Mechanically stacked tandem solar cells are a potential near-term solution for increasing the efficiency of photovoltaic modules. Practical implementation requires an interconnection approach that maximizes efficiency and minimizes complexity and cost. Connecting the top and bottom cells in a voltage-matched configuration allows two-terminal modules to be fabricated without altering the cell design or processing methods. Here, we experimentally demonstrate two-terminal voltage-matched $GaInP_2/Si$ minimodules. The two-terminal minimodules performed just as well as four terminal configurations when voltage-matching requirements were met. The magnitude of the efficiency loss experienced by the voltage-matched minimodule when voltage-matched conditions were not met depends on whether the voltage was constrained by the $GaInP_2$ or Si cells. Monte Carlo simulations also indicate that the two-terminal voltage-matched tandems respond to small cell-to-cell parameter variations in a similar manner as four terminal tandems. © *2018 Society of Photo-Optical Instrumentation Engineers (SPIE)* [DOI: 10.1117/1.JPE.8.045504]

Keywords: tandem solar cell; voltage matched; photovoltaics.

Paper 18124 received Oct. 11, 2018; accepted for publication Dec. 6, 2018; published online Dec. 31, 2018.

1 Introduction

Tandem architectures are regarded as a next step to realizing substantial efficiency gains in photovoltaic (PV) modules.[1–3] Energy production at higher areal densities is a key approach for driving down balance of systems costs, and it can also enable the use of PV in space-constrained applications. The main challenge is to make tandem modules that are cost-effective compared to single junction technologies that already dominate the market (e.g., multi- and monocrystalline Si and CdTe).[4–6] To this end, mechanical stacking of existing PV technologies (including Si, III-V, and thin film materials) offers a pathway to near-term implementation while drawing on demonstrated advantages in cost and scalability.

Practical realization of tandems hinges on the development of methods to interconnect cells that maximize efficiency and lower manufacturing and installation costs. Leaving the tandem as a four-terminal (4T) device allows it to reach its highest possible performance under any condition because the cells operate independently.[7] The drawback is that 4T operation deviates from the standard two-terminal (2T) designs, which may increase system and installation complexities. For example, multiple inverters may need to be used, additional connections must be made during installation or the interlayers between stacked but independently operating strings of cells may need to be robust enough to resist breakdown when those strings are operated under much different voltages. Replicating existing 2T system designs and installation methods requires the addition of a constraint. Current-matched designs, where stacked top and bottom cells are

*Address all correspondence to Kirstin Alberi, Kirstin. Alberi@nrel.gov

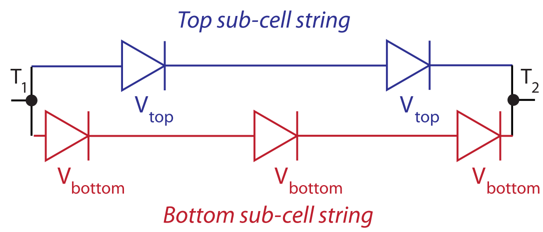

Fig. 1 Generalized schematic of a two-terminal VM tandem module.

connected in electrical series, constrain the current to that of the lowest-performing cell.[7,8] This approach generally places limitations on the combination of cell bandgap energies and cell thickness and/or area to achieve current matching.[8,9] Low resistance, transparent interconnections between an arbitrary combination of crystalline or polycrystalline materials can also be difficult to manufacture. On the other hand, voltage-matched (VM) designs, in which strings of top and bottom cells are connected in parallel, constrain the voltage to that of the lowest-performing string, and remove the need for low resistance electrical conduction between the dissimilar semiconductors.[7] Since the voltage of the strings can be fine-tuned by carefully selecting the number of cells they contain, this condition can be met in a straightforward way without altering the cell design or forming transparent conducting interconnections. Thus, such an approach offers design flexibility while also retaining the virtues of 2T system installations.

Various VM module designs have already been evaluated theoretically in the literature.[7,10–14] The general layout is presented in Fig. 1, where strings of serially connected top cells and strings of serially connected bottom cells are combined in parallel to form a 2T device. For each combination of PV technologies, there is an optimal ratio of bottom cells connected in series to top cells connected in series (bottom/top cell ratio) that is required to achieve VM conditions:

$$n_{\text{top}} V_{\text{mp,top}} = n_{\text{bottom}} V_{\text{mp,bottom}}.$$

Previous simulations have shown that 2TVM tandem modules can operate at high efficiencies over a wide range of bandgap combinations[7,10] and are much less susceptible to spectral variations than 2TCM designs due to the insensitivity of the max power voltage (V_{mp}) to photogenerated carrier density relative to the max power current. However, the VM tandem concept has yet to be thoroughly evaluated experimentally.

In this paper, we present an experimental demonstration of 2TVM minimodules using a mechanically stacked $GaInP_2/Si$ tandem as a model system. We have selected this combination of top and bottom cells based on its high potential efficiency and the ability to fabricate top cells with transparent back contacts. The experimental results here also build on previous simulations of $GaInP_2/Si$ tandems.[13] Our results show that 2TVM tandems can perform nearly as well as 4T configurations for small voltage mismatches below ∼20% and that they generally replicate simulated trends in performance as a function of bottom/top cell ratio. Given that our minimodules contain some cell-to-cell performance variations, we also evaluate the role of this variation in the overall module performance.

2 Experimental Methods

Minimodules were fabricated out of mechanically-stacked $GaInP_2$ and Si cells. $GaInP_2$ device layers were epitaxially grown in an upright configuration in a Veeco K475i metal-organic chemical vapor deposition (MOCVD) reactor using trimethylgallium, trimethylindium, trimethylaluminum, arsine, phosphine, disilane, diethyltellurium, dimethylzinc, and carbon tetrabromide precursor gases. The substrates were p-type (001) GaAs wafers offcut 5 deg toward the $\langle 011 \rangle$ direction, and the base thickness of the cells was ∼900 nm. Individual cells (2.52 cm^2) were fabricated in a superstrate configuration by affixing the upright device stack to a glass substrate with transparent epoxy and chemically removing the GaAs substrate. Front and back contacts were fabricated with electroplated Au, and ZnS/MgF_2 antireflection coatings were added to the front and back of each cell.

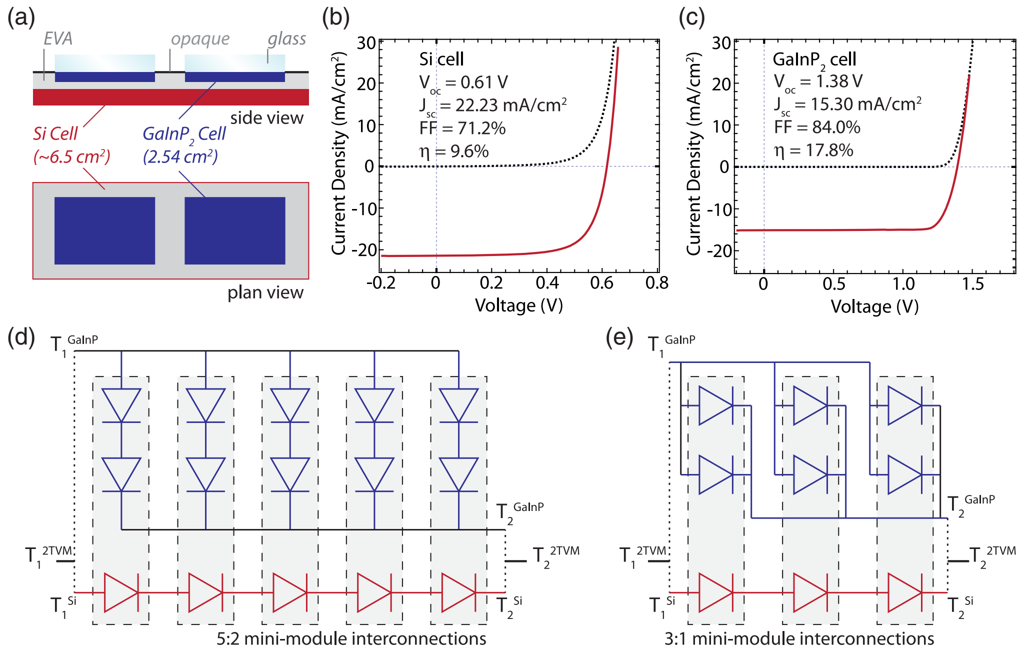

Fig. 2 Details of minimodules. (a) Schematic of a unit of two $GaInP_2$ cells mechanically stacked on a single Si cell (plan and side views). Light (solid) and dark (dotted) JV curves of representative (b) Si and (c) $GaInP_2$ cells measured at 25°C and 1 sun conditions. Interconnection schemes of (d) 5:2 and (e) 3:1 2TVM tandem minimodules. The terminals of the GaInP strings (T_1^{GaInP} and T_2^{GainP}) and Si strings (T_1^{Si} and T_2^{Si}) are labeled. Those terminals are connected together (via the dotted lines) to form the 2TVM tandem.

Interdigitated back contact Si cells were fabricated from high lifetime Si wafers. N-type and p-type amorphous Si (a-Si) was patterned over an intrinsic a-Si layer to form the backside heterojunctions. A front-surface field was formed with intrinsic and p-type a-Si layers, and it was finished with a low temperature-grown SiN_x coating. The wafer-sized devices were then sectioned into cells $\sim$1.5 cm $\times$ 6 cm.

Two $GaInP_2$ cells were mechanically stacked onto each Si cell with an ethylene-vinyl acetate (EVA) interlayer to form a single unit, as depicted in Fig. 2(a). Because the size of the Si cells routinely fabricated by our team was larger than twice the total area of the $GaInP_2$ cells we routinely fabricate, some areas at the edges of the Si cell were still exposed after stacking. The remaining area of the Si cell extending beyond the $GaInP_2$ cells [gray area in Fig. 2(a)] was covered with an opaque coating such that the total aperture area of the Si cell in each unit was 5.04 cm^2. Current–voltage (JV) curves for representative $GaInP_2$ and Si cells measured after the construction of these units are shown in Figs. 2(b) and 2(c). These units were then interconnected into strings to achieve various bottom/top cell ratios. We define the bottom/top cell ratio for each minimodule as the number of serially connected bottom cells in a string to the number of serially-connected top cells in a string (reduced to the lowest common terms). Two of the minimodule designs are shown in Figs. 2(d) and 2(e). Details of all minimodules are included in Table 1. Efficiencies of the 4T configurations were determined by adding the efficiencies of the independently operated $GaInP_2$ and Si strings. These strings were then connected in parallel to obtain the efficiency of the 2TVM tandem.

3 Experimental Results

Previous simulations of 2TVM $GaInP_2$/Si tandems indicated that a 5:2 ratio is nearly optimal for this PV technology combination.[13] We therefore tested four bottom/top cell ratios around this value: 4:1, 3:1, 5:2, and 2:1. The JV curves of the $GaInP_2$ string, Si string, and 2TVM device of the tandem with the 5:2 ratio are plotted in Fig. 3(a). The efficiencies of the 2TVM and 4T configurations for all four bottom/top cell ratios are shown in Fig. 3(b), and the corresponding

Table 1 Minimodule configurations and characteristics. Measured parameters include the open circuit voltage, V_{oc}, max power voltage, V_{mp}, short-circuit current density, J_{sc}, fill factor, FF, and efficiency, η. The efficiencies of the individual $GaInP_2$ and Si string measurements are added together to obtain the 4T module efficiencies.

Bottom/top cell ratio	Area (cm^2)	String configurations		V_{oc} (V)	V_{mp} (V)	J_{sc} (mA/cm^2)	FF (%)	η (%)
4:1	20.16	GaInP	Eight GaInP cells connected in parallel	1.37	1.13	15.01	77.8	16.0
		Si	Four Si cells connected in series	2.41	1.93	4.60	69.9	7.7
		2TVM	GaInP and Si strings connected in parallel	1.41	1.16	19.54	78.5	21.6
3:1	15.12	GaInP	Six GaInP cells connected in parallel	1.38	1.18	15.14	81.0	16.9
		Si	Three Si cells connected in series	1.81	1.40	6.10	70.0	7.7
		2TVM	GaInP and Si strings connected in parallel	1.41	1.18	21.27	79.9	23.9
5:2	25.20	GaInP	Five sets of 2 GaInP cells connected in series. The five sets are then connected in parallel	2.76	2.34	7.20	81.05	16.1
		Si	Five Si cells connected in series	3.03	2.36	3.49	69.56	7.4
		2TVM	GaInP and Si strings connected in parallel	2.82	2.34	10.69	77.88	23.4
2:1	20.16	GaInP	Four sets of 2 GaInP cells connected in series. The four sets are then connected in parallel	2.76	2.39	7.37	82.8	16.9
		Si	Four Si cells connected in series	2.42	1.83	4.54	66.6	7.3
		2TVM	GaInP and Si strings connected in parallel	2.65	2.05	11.89	68.6	21.6

efficiency differences are shown in Fig. 3(c). Each of the minimodules was fabricated with a different number of cells and total area (noted in Table 1) to achieve the targeted bottom/top cell ratio. The performances of the individual cells also deviated from one another slightly as a result of normal processing variations. These two factors are the main source of the differences in the 4T efficiencies. We therefore focus mostly on the differences between the efficiencies of the 4T and 2TVM configurations for each bottom/top cell ratio. However, we note that all $GaInP_2$ strings exhibited efficiencies of 16%, all Si strings exhibited efficiencies of 7%, and all 4T minimodules exhibited efficiencies within 1% absolute of one another. These reasonable string efficiencies combined with the small deviation in the 4T minimodule efficiencies provide some confidence that a single factor (e.g., the performance of a single outlier cell or string) has not altered the trends in the 4T versus 2TVM tandem performances. More discussion on the impact of cell-to-cell variations is included later in the text.

A bottom/top cell ratio of 5:2 for our mechanically stacked $GaInP_2/Si$ tandem produced nearly voltage-matched conditions, which is consistent with previous simulations.[13] The V_{mp} values of the $GaInP_2$ and Si strings within the 5:2 minimodule are marked on the JV curves in Fig. 3(a). They are within 0.02 V of each other, and the V_{mp} value of the 2TVM tandem is pinned at the lower V_{mp} of the two (the $GaInP_2$ string). The 4T and 2TVM tandem efficiencies are within 0.1%. The difference between the 4T and 2TVM tandem efficiencies widens at higher and lower bottom/top cell ratios. For a bottom/top cell ratio of 3:1, where the V_{mp} of the Si string is 19% higher than the V_{mp} of the $GaInP_2$ string, the efficiency drops by ~0.7% when using a 2TVM configuration. An even higher bottom/top cell ratio of 4:1 produces a larger efficiency drop of 2.1% for a voltage mismatch of 70%. On the other hand, the V_{mp} of the $GaInP_2$ string is ~30% greater than that of the Si string when the bottom/top cell ratio is lowered to 2:1. However, the efficiency of the 2TVM configuration of that tandem is ~2.5% lower than the 4T configuration. These results suggest that there is an asymmetry in the efficiency loss exhibited by the 2TVM tandem depending on whether the V_{mp} of the top or bottom cell strings is higher.

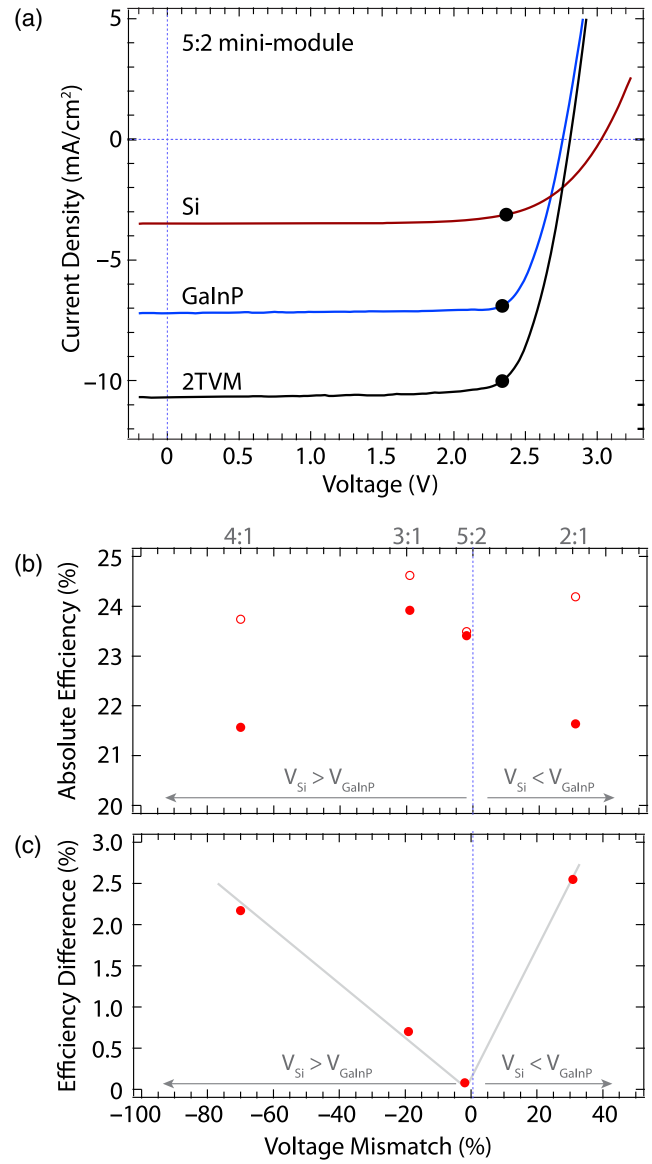

Fig. 3 Experimental results of the 5:2 minimodule. (a) JV curves for the Si and $GaInP_2$ strings and the resulting 2TVM tandem. The solid dots mark the V_{mp} values of each curve. (b) Efficiencies of the 4T (open circles) and 2TVM (closed circles) of the 4:1, 3:1, 5:2 and 2:1 tandems. (c) Differences in the efficiencies between the 4T and 2TVM configurations for each tandem in (b). Solid gray lines are guides to the eye for trends in the efficiency differences as a function of voltage mismatch when the V_{mp} for the bottom Si strings are greater than or less than the V_{mp} of the $GaInP_2$ strings.

Such an asymmetry can be expected when the tandem is pinned by either the bottom or top cells in the limiting case.[15] Because the $GaInP_2$ string has a higher efficiency than the Si string, the efficiency of the 2TVM tandem will decrease by a smaller amount when it is limited by the $GaInP_2$ string than the Si string. However, many more data points are needed to experimentally establish accurate trends.

4 Simulations

Commercial modules are typically constructed from cells that are binned for uniformity in performance. However, the cells used in these experimental modules exhibited a degree of

Table 2 Parameters used in minimodule simulations.

	GaInP cells		Si cells	
Parameter	Maximum value	Minimum value	Maximum value	Minimum value
Log (J_0)	−10.53	−13.40	−8.80	11.80
n	2.63	1.95	1.40	1.00
J_{sc} (mA/cm^2)	15.69	14.93	18.75	18.37
R_s (ohm/cm^2)	3.93	1.02	1.40	0.27
R_{sh} (ohm/cm^2)	6.76×10^4	4.96×10^3	1.08×10^3	5.20×10^2

nonuniformity that could be expected from variations associated with processing small batches of cells at a laboratory scale. We were therefore interested in understanding the role of these variations in the overall 2TVM efficiency. Here, we present the results of simulations of 4T and 2TVM tandems constructed of cells exhibiting different ranges of parameters.

The JV curves of our experimental cells were first fit with the diode equation to extract the short circuit current, J_{sc}, dark current, J_0, diode ideality parameter, n, series resistance, R_s, and shunt resistance, R_{Sh}, for each:

$$J = -J_{\mathrm{sc}} + J_0 \exp\left(\frac{V - JR_{\mathrm{s}}}{nkT}\right) + \frac{V}{R_{\mathrm{Sh}}}.$$

The range, R, between the minimum and maximum values of each of these parameters, P, was established as $R = P_{\max} - P_{\min} = \Delta P$ (values are noted in Table 2). We then either doubled ($R = 2\Delta P$) or halved ($R = 0.5\Delta P$) that range according to the methodology presented in Fig. 4(a). Parameters J_0 and n were found to be correlated and were treated as such in the simulations. Logarithmic values of J_0 were also used to assess the range for this parameter in order to meaningfully vary R. For all other parameters, the distributions were chosen to be "pessimistic" (i.e., always limited by the best experimentally measured value).

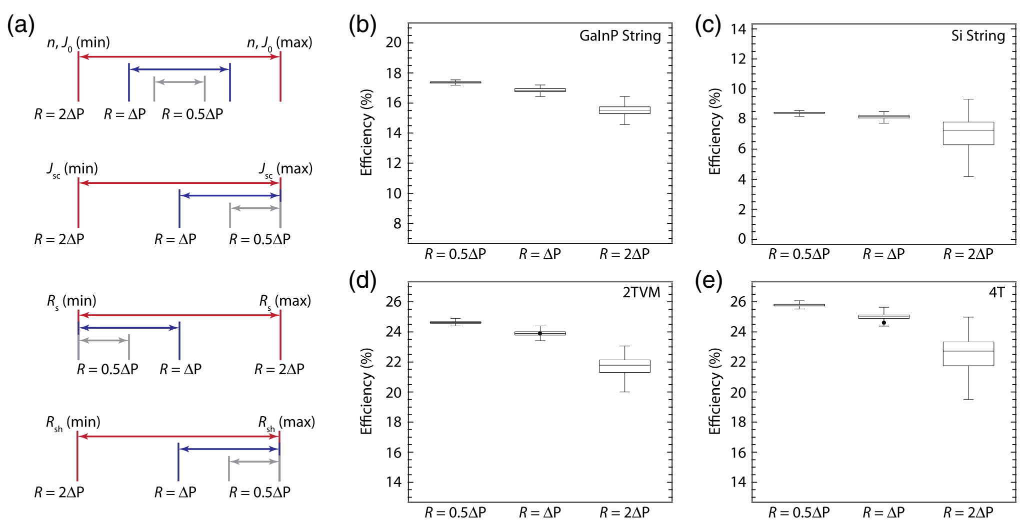

Fig. 4 Results of 3:1 minimodule simulations. (a) Schematic of how the parameter ranges, P, were varied for the simulations. Efficiencies are plotted for all three P ranges for (b) the $GaInP_2$ string, (c) the Si string, (d) the 2TVM tandem, and (e) the 4T tandem. The circular markers in (d) and (e) represent the experimentally-measured module values.

Using these parameter distributions, we simulated tandems with the 3:1 design used in our experimental minimodule [see Fig. 2(e)] to model the case, where VM conditions are not met. A Monte Carlo algorithm was used to generate variations in the circuit components by fitting a random distribution across the different R ranges defined already. Multiple simulations (500) were run to generate a statistical analysis of the JV output. The efficiencies of the $GaInP_2$ and Si strings and the resulting 4T and 2TVM tandems are shown in Figs. 4(b)–4(e).

As expected, the full range of simulated efficiencies increases and the median values decrease as P increases from 0.5 to 2 for all cases. Variations in individual cell short-circuit currents, diode ideality factors and series resistances over the ranges studied here had the most effect on the minimodule efficiency. As making any of these parameters substantially worse for one cell in a series-connected string can lower the J_{sc}, V_{oc}, and/or FF of that string, the efficiencies of both the 4T and 2TVM configurations will also decrease relative to the case where all cells have the best parameter value. The differences between the $R = 0.5\Delta P$ and $R = \Delta P$ distributions are not very large, but there is a substantial change between $R = \Delta P$ and $R = 2\Delta P$. The key takeaway from these simulations is that the distribution of parameters found in our experimental cells ($R = \Delta P$) likely does not greatly impact the performance of the 4T or 2TVM tandems other than to slightly reduce their efficiencies compared to instances where the cells have been binned for tighter tolerances in all parameters. The distribution of efficiencies around the median value in each case is still quite small. We note here that the experimental efficiencies for the 4T and 2TVM tandems align well with the simulated values [marked in Figs. 4(d) and 4(e)]. The efficiency differences between those configurations therefore match quite well between the simulated and experimental values. There is also little change in the expected efficiency differences between and the $R = 0.5\Delta P$ and $R = \Delta P$ distributions. However, a wider distribution of parameters similar to $R = 2\Delta P$ is expected to produce a much larger drop in performance.

5 Discussion

Our experimental demonstration indicates that mechanically stacked 2TVM tandem module designs can compete with 4T designs with minimal modifications to the individual cells. Provided that the top and bottom cell strings are designed to have V_{mp} values within 10% to 20% of each other, the 2TVM tandem will operate very close to the efficiencies of the 4T configuration. We have experimentally demonstrated this concept here with a $GaInP_2/Si$ tandem, but it can be applied to any combination of PV technologies.[16,17] The ideal bottom/top cell ratio of course will depend on the PV technologies that make up each junction, and it will also depend to a smaller degree on the operating temperature of the module.[13] However, achieving a desired bottom/top cell ratio can be straightforward through mechanical stacking. Because the cells can be fully fabricated before integration on either side of an insulating layer (as carried out in this work using a sheet of EVA), the top and bottom cells do not need to conform to one another in terms of size, number, or tiling design. The number of top cell strings also does not need to equal the number of bottom cell strings; only their V_{mp} values must match. This level of design freedom opens up possibilities for stacking superstrate thin film modules directly on Si modules or using innovative methods for cost effectively integrating III–V cells into tandems, for example.[16,18] In cases where achieving the ideal bottom/top cell ratio is difficult, we have previously shown that adding a module-level DC-DC buck converter to bottom cell strings designed with a higher V_{mp} than the top cell strings will automatically produce VM conditions in a range of operating environments.[13] Thus, 2TVM tandem module designs can take advantage of conventional PV module fabrication methods, system designs, and installation practices while retaining 4T efficiencies.

6 Conclusion

In summary, we have experimentally demonstrated the 2TVM concept. Using $GaInP_2/Si$ minimodules, we showed that 2TVM configurations can exhibit the same efficiency as 4T configurations if the top and bottom cell strings are designed to have the same V_{mp} values.

An asymmetry in the efficiency loss if the top or bottom string has a lower V_{mp} indicates that any voltage mismatch should be accommodated by designing the bottom string with a higher V_{mp}. Monte Carlo simulations of 2TVM and 4T tandems indicate that both tolerate small-scale cell-to-cell variations in a similar way before the module performance starts to substantially degrade with increasing spread in cell parameters. 2TVM designs therefore offer a practical method for implementing tandems at the module level.

Acknowledgments

This work was authored in part by the National Renewable Energy Laboratory, operated by Alliance for Sustainable Energy, LLC, for the U.S. Department of Energy (DOE) under Contract No. DE-AC36-08GO28308. Funding was provided by U.S. Department of Energy Office of Energy Efficiency and Renewable Energy Solar Energy Technologies Office. The views expressed in the article do not necessarily represent the views of the DOE or the U.S. government. The U.S. government retains and the publisher, by accepting the article for publication, acknowledges that the U.S. Government retains a nonexclusive, paid-up, irrevocable, worldwide license to publish or reproduce the published form of this work, or allow others to do so, for U.S. government purposes.

References

1. M. A. Green, "Commercial progress and challenges for photovoltaics," *Nat. Energy* **1**, 15015 (2016).
2. Z. Yu, M. Leilaeioun, and Z. Holman, "Selecting tandem partners for Si solar cells," *Nat. Energy* **1**, 16137 (2016).
3. S. Essig et al., "Raising the one-sun conversion efficiency of III-V/Si solar cells to 32.8% for two junctions and 35.9% for three junctions," *Nat. Energy* **2**, 17144 (2017).
4. S. U. Nanayakkara et al., "Evaluating the economic viability of CdTe/CIS and CIGS/CIS tandem photovoltaic modules," *Prog. Photovoltaics Res. Appl.* **25**, 271–279 (2017).
5. D. Bobela et al., "Economic competitiveness of III-V on silicon tandem one-sun photovoltaic solar modules in favorable future scenarios," *Prog. Photovoltaics Res. Appl.* **25**, 41–48 (2017).
6. I. M. Peters et al., "Techno-economic analysis of tandem photovoltaic systems," *RSC Adv.* **6**, 66911–66923 (2016).
7. J. M. Gee, "A comparison of different module configurations for multi-band-gap solar cells," *Sol. Cells* **24**, 147–155 (1988).
8. S. R. Kurtz, P. Faine, and J. M. Olson, "Modeling of two-junction, series-connected tandem solar cells using top-cell thickness as an adjustable parameter," *J. Appl. Phys.* **68**, 1890–1895 (1990).
9. J. Yang et al., "Fabrication of high-efficiency III-V on silicon multijunction solar cells by direct metal interconnect," *IEEE J. Photovoltaics* **4**, 1149–1155 (2014).
10. R. Strandberg, "Detailed balance analysis of area de-coupled double tandem photovoltaic modules," *Appl. Phys. Lett.* **106**, 033902 (2015).
11. A. Lentine et al., "Enhanced efficiency for voltage matched stacked multi-junction cells: optimization with yearly temperature and spectra variations," in *IEEE 39th Photovoltaic Specialists Conf.*, pp. 788–790 (2013).
12. A. Lentine et al., "Voltage matching and optimal cell compositions for microsystem-enabled photovoltaic modules," *IEEE. J. Photovoltaics* **4**, 1593–1602 (2014).
13. S. MacAlpine et al., "Simulated potential for enhanced performance of mechanically stacked hybrid III-V/Si tandem photovoltaic modules using DC-DC converters," *J. Photonics Energy* **7**, 042501 (2017).
14. H. Schulte-Huxel, D. J. Friedman, and A. C. Tamboli, "String-level modeling of two, three, and four terminal Si-based tandem modules," *IEEE J. Photovoltaics* **8**, 1370–1375 (2018).
15. D. Bobela et al., "Demonstration of GaInP2/Si voltage-matched tandem solar cells," in *IEEE 44th Photovoltaic Specialists Conf. (PVSC)* (2017).

16. A. C. Tamboli et al., “Low-cost CdTe/silicon tandem solar cells,” *IEEE J. Photovoltaics* **7**, 1767–1772 (2017).
17. D. P. McMeekin et al., “A mixed-cation lead mixed-halide perovskite absorber for tandem solar cells,” *Science* **351**, 151–155 (2016).
18. M. P. Lumb et al., “Towards the ultimate multi-junction solar cell using transfer printing,” in *IEEE 43rd Photovoltaic Specialist Conf. (PVSC)* (2016).

Biographies of the authors are not available.